In Vitro and In Vivo Recording of Local Field Potential Oscillations in Mouse Hippocampus

L.H. Forsyth,[1] J. Witton,[2] J.T. Brown,[2] A.D. Randall,[2] and M.W. Jones[1]

[1]School of Physiology and Pharmacology, University of Bristol, Bristol, United Kingdom
[2]Pfizer Applied Neurophysiology Group, School of Physiology and Pharmacology, University of Bristol, Bristol, United Kingdom

ABSTRACT

Oscillations in hippocampal local field potentials (LFP) reflect the coordinated, rhythmic activity of constituent interneuronal and principal cell populations. Quantifying changes in oscillatory patterns and power therefore provides a powerful metric through which to infer mechanisms and functions of hippocampal network activity at the mesoscopic level, bridging single-neuron studies to behavioral assays of hippocampal function. Here, complementary protocols that enable mechanistic analyses of oscillation generation in vitro (in slices and a whole hippocampal preparation) and functional analyses of hippocampal circuits in behaving mice are described. Used together, these protocols provide a comprehensive view of hippocampal phenotypes in mouse models, highlighting oscillatory biomarkers of hippocampal function and dysfunction. *Curr. Protoc. Mouse Biol.* 2:273-294 © 2012 by John Wiley & Sons, Inc.

Keywords: theta rhythm • gamma rhythm • electrophysiology • LFP • slice • in vitro • in vivo

INTRODUCTION

Its laminar arrangement of synaptic and cellular layers plus a wealth of anatomical, neurophysiological, and behavioral data mean that the rodent hippocampus is an experimentally tractable model system in which to define the neuronal network bases of learning and memory by linking the properties of its constituent cell types to population-level local field potential (LFP) activity and behavioral output (Klausberger and Somogyi, 2008). This is particularly powerful in combination with cell type-selective manipulations in genetically altered mouse lines (e.g., Korotkova et al., 2010), and may also be used to identify biomarkers and infer mechanisms of network dysfunction in models of disease (Arguello and Gogos, 2006).

LFP are extracellular voltages generated by the population activity of electrically excitable cells in the vicinity of a recording electrode placed into brain tissue; coordinated, rhythmic activity in these populations gives rise to LFP oscillations. Thus, the basis of LFP generation bears much in common with that of electroencephalography (EEG), but the use of invasive microelectrodes allows measurement of more localized, spatially-weighted averages of activity in defined neural networks. Interpretation of LFP signals can nevertheless be complex, with parameters such as spatial extent and timecourse varying considerably across different brain regions and electrode types (see Commentary).

Here, techniques for recording hippocampal network LFP oscillations in mouse hippocampus using the following three contrasting but complementary experimental approaches are described: (1) pharmacological induction of gamma (30 to 100 Hz) oscillations in CA3 of acute hippocampal slices; (2) recording spontaneous theta (5 to 10 Hz)

Published online September 2012 in Wiley Online Library (wileyonlinelibrary.com).
DOI: 10.1002/9780470942390.mo120089

oscillations in CA1 of acutely-isolated whole hippocampus in vitro; and (3) recording in vivo network activity in freely behaving mice.

All procedures must be approved by local and/or national ethical guidelines and legislation for use of animals in research, and veterinary advice should be sought before initiating in vivo experiments.

BASIC PROTOCOL 1

PRODUCING HIPPOCAMPAL SLICES

Horizontal and transverse hippocampal slice production is described below.

Materials

Mice
High-sucrose cutting solution (see recipe), ice-cold
Carbogen (95% O_2/5% CO_2) source
Quick drying superglue (cryanoacylate)
aCSF (see recipe)
Agar block (~15 × 15 × 10–mm)

Large surgical scissors
Scalpel with no. 11 blade
Vannas micro scissors/small surgical scissors
Dumont no. 7 forceps
Small spatulas
Small teaspoon
Filter paper
10-cm diameter Petri dishes
Medium spatula
Vibrating microtome
Pasteur pipet
Slice incubation chamber
Razor blades

Euthanize animal and remove brain

1. Scruff the mouse to restrain it and place onto a flat work surface. Euthanize via cervical dislocation. In a single, rapid movement, place large scissors between shoulder blades and base of the skull. Compress the spine. Without moving the scissors, pull sharply on the tail to dislocate the spine.

2. Remove skull from the body using the large scissors to cut through the neck at the point of dislocation.

3. Hold the snout and use the no. 11 scalpel to cut the skin overlying the dorsal surface of the skull. Peel the skin away laterally from the midline to expose the dorsal skull.

   Make a single smooth cut along the midline, starting at the rostral end of the skull at a point between the eyes and moving to the caudal end of the skull.

4. Use the micro scissors/small scissors to cut along the midline of the skull to the point at which the frontal cortex meets the olfactory bulb. Use the curved Dumont no. 7 forceps to peel away the skull covering each hemisphere.

   Make small, progressive cuts in the bone. Start at the caudal end of the skull and move in the rostral direction. Care should be taken to ensure that the brain is not damaged by the scissor blades. Pull back the skull laterally from the midline to expose the dorsal surface of the brain.

Prepare slices

For horizontal slices

5a. Insert the small spatula between the frontal cortex and olfactory bulb. Gently lift the brain out of the skull along the caudal-dorsal axis and immediately place into ice-cold cutting solution bubbled with carbogen. Allow to recover for ∼30 sec.

6a. Use a small teaspoon to remove brain from the cutting solution and transfer onto filter paper moistened with cutting solution on an ice-filled Petri dish.

The Petri dish can be used as a rotatable stage.

7a. Remove the cerebellum with a single scalpel cut.

8a. Place a drop of superglue onto the microtome stage and stick the brain onto it in an inverted position.

The ventral surface of the brain should be facing vertically upwards, away from the stage.

9a. Place the stage into the vibrating microtome. Immediately cover the brain in ice-cold cutting solution and gently bubble with carbogen.

The cutting solution should not be poured directly onto the brain. Large chunks of ice should also be avoided.

10a. Cut the brain into 400-μm sections.

11a. Use a Pasteur pipet to transfer the sections to a Petri dish containing aCSF gently bubbled with carbogen.

12a. Use a precise scalpel cut to separate the hemispheres.

The hippocampus may also be isolated from the rest of the brain slice using scalpel cuts.

13a. Use a Pasteur pipet to transfer sections to a slice incubation chamber filled with carbogen bubbled aCSF.

14a. Incubate slices 30 min at 37°C.

15a. Return slices to room temperature.

The slices may remain incubated under these conditions for the rest of the experimental period.

For transverse slices

To produce transverse slices, the intact hippocampus must first be removed from each brain hemisphere and then sliced across its transverse axis. Steps to produce transverse slices are also depicted in Figure 1.

5b. With the exposed brain still in the cranium, use precise scalpel cuts to remove the cerebellum and frontal cortex and separate the brain along the midline into two hemispheres. Gently lift the hemispheres out of the skull along the caudal-dorsal axis and immediately place into ice-cold cutting solution bubbled with carbogen. Allow to recover for ∼30 sec.

6b. Use a small teaspoon to remove a brain hemisphere from the cutting solution and transfer onto filter paper moistened with cutting solution on an ice-filled Petri dish.

The Petri dish can be used as a rotatable stage.

7b. Position the hemisphere on its frontal cortex. Use a small spatula to support the internal region of medial dorsal cortex.

This spatula provides support and leverage to facilitate hippocampal exposure and removal from the surrounding cortex.

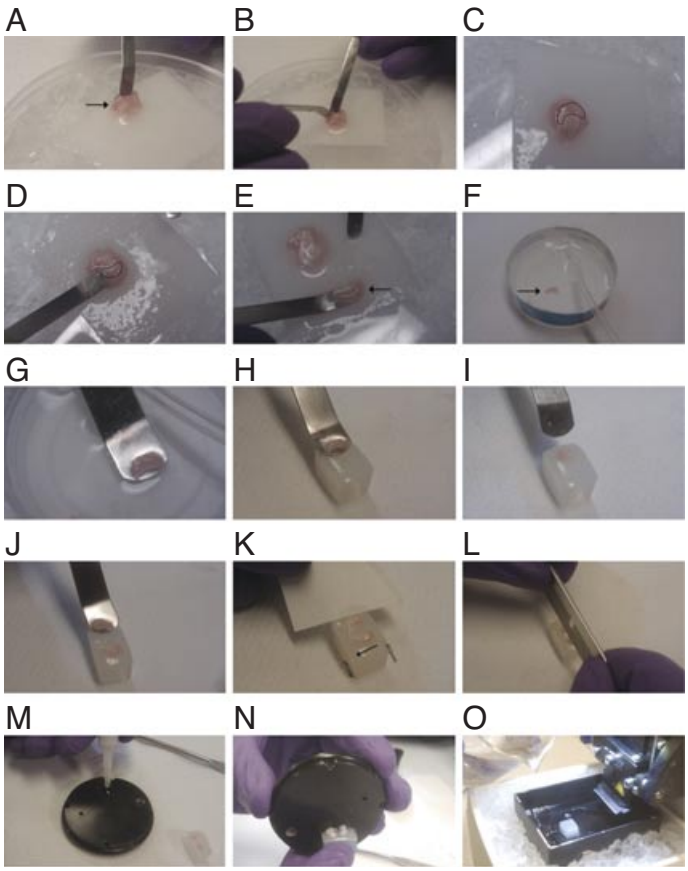

Figure 1 Hippocampal isolation and generation of transverse slices. (**A**) The brain hemisphere (arrow) is placed on its frontal cortex and a spatula is used to support the medial dorsal cortex. (**B**) A second spatula is used to gently peel away the brainstem and thalamus. (**C**) The hemisphere following B. The exposed hippocampus is outlined in black. (**D**) Isolate the hippocampus (outlined in black) by sliding a spatula between the extreme dorsal surface of the hippocampus and the surrounding cortex. (**E**) The isolated hippocampus (arrow). (**F**) Place the hippocampal isolate (arrow) into a shallow vessel containing ice-cold cutting solution and gently bubble with carbogen. Repeat A through F on the second brain hemisphere. (**G**) Use a large spatula to lift the hippocampus from the cutting solution. CA1/CA3 should be facing downwards and the dentate gyrus/subiculum facing vertically upwards. (**H**–**I**) Position the spatula above the flat surface of an agar block. Rotate 180° and place the hippocampus onto the agar block with the dentate gyrus/subiculum facing downwards. (**J**-**K**) Repeat H through I for the second hippocampal isolate. The hippocampus should be positioned on the block such that the extreme dorsal and ventral ends of the two hippocampi are side by side (arrow). Use a small piece of filter paper to remove excess cutting solution. (**L**) Use a razor blade to make a vertical cut through the extreme ventral end of the hippocampi and agar block. (**M**) Place a dab of superglue on the microtome stage. (**N**) Glue the cut end of the hippocampi and agar block to the microtome stage. Try to avoid getting glue on the hippocampal tissue. Holding the stage vertically should help with this. (**O**) Place the stage into the vibrating microtome and cover with ice cold cutting solution.

8b. Use an additional small spatula to peel away the brainstem and thalamus to expose the hippocampus.

9b. Dissociate the hippocampus from the surrounding cortex. To do this, place the second spatula between the extreme dorsal portion of the hippocampus and the surrounding cortex. Move the spatula smoothly through the cortex caudal to the hippocampus.

10b. Use the micro scissors to trim any cortex remaining on the hippocampal isolate. Place the hippocampal isolate into a small vessel containing ice-cold cutting solution gently bubbled with carbogen.

Hippocampal isolation from the hemisphere should be completed within ∼1 min to minimize neuronal death.

11b. Repeat steps 6b to 10b on the second brain hemisphere.

12b. Use a medium spatula to transfer the hippocampi to the broad, flat surface of an agar block. To do this, slide the spatula beneath the CA1-CA3 region of the hippocampus, such that the dentate gyrus/subiculum face vertically upwards. Remove the hippocampus from the cutting solution and position the spatula above the agar block. Then rotate the spatula 180° and transfer the hippocampus onto the agar block such that dentate gyrus/subiculum lie on the agar and CA1-CA3 face vertically upwards. The two hippocampi should be positioned next to each other along the same longitudinal axis, such that the extreme dorsal and extreme ventral ends are side-by-side.

13b. Use a small piece of filter paper to remove excess cutting solution from the agar block.

14b. Use the razor blade to cut through and remove the extreme ventral end of the hippocampi and underlying agar block.

The cut should be perpendicular to the longitudinal axis of the hippocampi.

15b. Place a drop of superglue on the microtome stage and stick the cut end of the agar block onto it, such that the longitudinal axis of the hippocampi points vertically upwards.

Avoid getting excess glue on the hippocampal tissue, holding the stage vertically while gluing the agar block should help with this.

16b. Place the stage into the vibrating microtome. Immediately cover the tissue in ice-cold cutting solution and gently bubble with carbogen.

The cutting solution should not be poured directly onto the hippocampi. Large chunks of ice should also be avoided.

17b. Cut the hippocampi across their transverse axis into 400- to 500-μm sections.

18b. Use a Pasteur pipet to transfer the sections to a slice incubation chamber containing aCSF bubbled with carbogen.

19b. Incubate slices 30 min at 37°C.

20b. Return slices to room temperature.

The slices may remain incubated under these conditions for the rest of the experimental period.

PHARMACOLOGICAL INDUCTION OF GAMMA OSCILLATIONS

BASIC PROTOCOL 2

Gamma oscillations can be induced in CA3 by applying low concentrations of kainate (a potent AMPA and kainate receptor agonist) or carbachol (a non-selective muscarinic acetylcholine receptor agonist) to the hippocampal slices. Carbachol concentrations of 5 to 20 μM have been shown to induce gamma activity in rodent hippocampal slices (Fisahn et al., 1998; Vreugdenhil and Toescu, 2005; Oren et al., 2006; Mann and Mody, 2010). The authors have preferentially used kainate in their studies. However, the methodology is the same for both techniques and can be applied interchangeably.

The slice recording chamber and other hardware should be set up according to the manufacturers' instructions. To enhance signal-to-noise, the chamber should be fixed on an air-table and surrounded by a grounded Faraday cage. Electrical noise can be further reduced by grounding objects within the Faraday cage. A microscope should be used to visualize the recording chamber; for basic experiments a dissection microscope should be sufficient. A useful resource for troubleshooting in vitro electrophysiology rig set-up is provided by Axon Instruments, available for free download at *http://www.whitney.ufl.edu/BucherLab/techspecs/Axon_Guide.pdf*.

Materials

Reservoir of carbogenated aCSF (see recipe)
Carbogen (95% O_2/5% CO_2) source
Hippocampal slices (see Basic Protocol 1)
Kainate stock (e.g., 1 mM)

Slice recording chamber fixed on an air-table and surrounded by a grounded Faraday cage
Perfusion pump
Dissection microscope
Soft bristled no. 5 sable hair brush, optional
Small pieces of lens cleaning tissue (∼1-mm square; interface recording chamber only)
Slice weights (e.g., short pieces (2- to 3-mm long) of twisted silver wire; submerged recording chamber only), optional
Pasteur pipet
Glass microelectrodes (pulled from borosilicate glass capillaries, <1-mm diameter, to a resistance of 2 to 5 mΩ)
Microfil and 1-ml syringe
Sliver wire recording electrode connected to a headstage pre-amplifier
Micromanipulator
Water bath
Amplifier
Hum Bug noise eliminator
Analog-to-digital signal converter
Personal computer with electrophysiology data acquisition software

1. Use the perfusion pump to continuously perfuse the recording chamber with carbogenated aCSF maintained at 33° ± 2°C by an internal heater.

   The aCSF reservoir should also be maintained at 33° ± 2°C in the water bath.

   The required perfusion speed will be determined by the type of recording chamber.

2. Remove a hippocampal slice from the incubation chamber and rapidly transfer it to the recording chamber under a dissection microscope.

   If using an interface chamber, transfer the slice to the recording chamber using bristles of a soft no. 5 sable hair paintbrush. Place a small square of lens cleaning tissue onto the synthetic mesh in the recording chamber. Gently slide the bristles under the slice and lift out of the incubation chamber. Position the bristles on top of the lens tissue and gently roll the paintbrush. The slice should slide off of the paintbrush and onto the lens tissue.

   If using a submerged chamber, carefully transfer the slice to the recording chamber using a Pasteur pipet. Position slice weights on the extreme edges of the slice to prevent movement from perfusion currents (do not place the weights on regions of the slice from which you intend to record).

3. Leave hippocampal slice to acclimatize in the recording chamber.

   For interface conditions, the slice should be left for ∼30 min. For submerged conditions, leave the slice for ∼5 to 10 min.

4. Semi-fill a glass microelectrode with aCSF using a microfil and 1-ml syringe. Connect to the silver wire recording electrode (the wire recording electrode must be in direct contact with the microelectrode solution).

   The silver wire electrode should be chloride coated —the authors recommend incubating the wire for several hours in household bleach to accomplish this. The recording electrode ensemble and headstage pre-amplifier should be fitted to a micromanipulator to facilitate accurate positioning of the recording electrode in the slice.

5. Use the micromanipulator to position the recording electrode in CA3 of the hippocampal slice.

   Gamma activity will vary across both the medial and longitudinal axes of CA3. Gamma power is strongest in the stratum radiatum. Gamma recorded in stratum radiatum will have opposite polarity to that recorded in stratum pyramidale. Gamma power has been reported to be strongest in CA3 nearest the hilus of the dentate gyrus (CA3c region) and to progressively decrease as the recording electrode is moved towards CA2 (CA3a region) (Vreugdenhil and Toescu, 2005). It is important to maintain consistent placement of the recording electrode across experiments.

6. Commence baseline data acquisition.

   The headstage pre-amplifier should be connected to a primary amplifier, which is connected in sequence to an analog-to-digital signal converter and data acquisition personal computer. Precisely how the extracellular signals are recorded will depend on the recording equipment used and experimental design. In the authors' experiments, the recorded signal is typically amplified 2000 times, band-pass filtered online between 0.5 Hz and 1.7 kHz, and digitized at a sampling frequency of 5 kHz. The recorded signal should be sampled continuously over the duration of the experiment.

   There are a variety of commercially available software packages for electrophysiology data acquisition; the authors typically use Clampex as part of the pCLAMP software suite (http://www.moleculardevices.com). A noise eliminator may be used to remove contaminating 50/60 Hz mains electricity noise from the pre-digitized signal. However, this is not necessarily required.

   It is advisable to record several minutes of continuous baseline activity before attempting to pharmacologically induce gamma oscillations. Hippocampal slices may display spontaneous gamma oscillations in CA3, although the authors have found this to be rare in transverse hippocampal slices.

7. Pharmacologically induce gamma oscillations in CA3 by applying kainate (50 to 500 nM) to the slice.

   Kainate should be delivered continuously to the whole slice via the perfusion solution. Add kainate stock at the appropriate concentration and volume directly to the heated aCSF reservoir.

   Note the emergence of a prominent 30- to 40-Hz oscillation in Figure 2A, ∼20 to 30 min post-kainate application. The gamma oscillation should have a saw-tooth-like appearance, with a fast ascending phase and slower descending phase (Fig. 2B).

8. Following collection of experimental data, complete analysis offline.

   The types of analyses that can be performed on pharmacologically induced gamma oscillations are similar to those for in vivo local field potentials. These are discussed in Basic Protocol 3 and Critical Parameters and Troubleshooting.

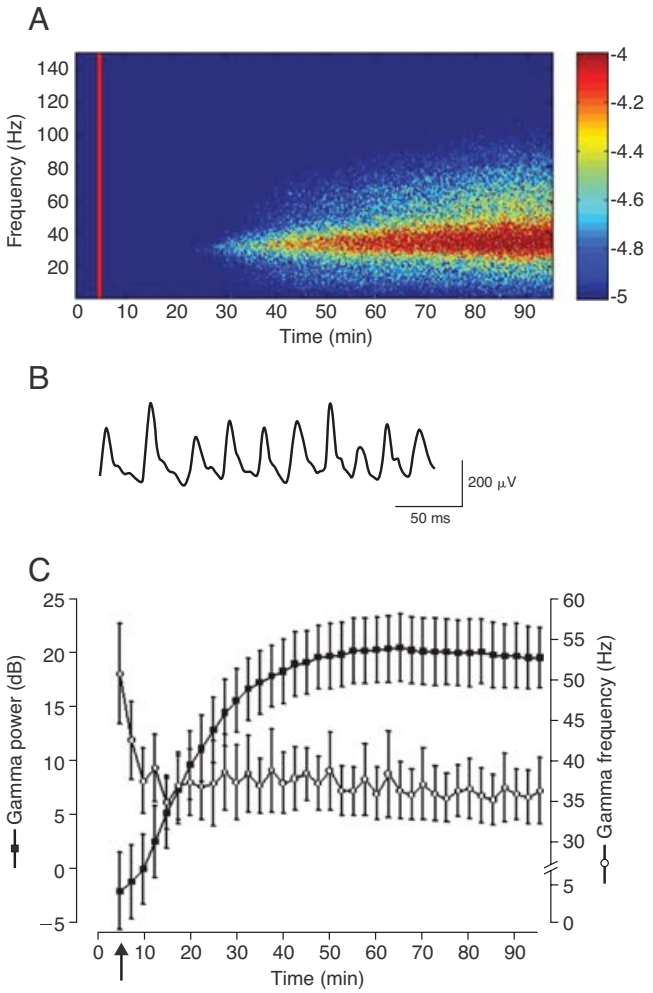

Figure 2 Kainate-induced gamma oscillations in transverse hippocampal slices. (**A**) Example spectrogram showing the development of gamma (30 to 100 Hz) oscillations in CA3 following the application of kainate (100 nM, red line) to a transverse hippocampal slice. (**B**) Example of steady-state gamma activity in (A) 80 min after kainate application. The raw trace has been filtered between 1 and 150 Hz. (**C**) Pooled data from six transverse hipppocampal slices. The figure plots the time-course of gamma oscillation generation after application of 100 nM kainate (arrow). Peak gamma band power (filled squares) and frequency (open circles) are plotted.

SUPPORT PROTOCOL

RECORDING SPONTANEOUS THETA OSCILLATIONS IN AN IN VITRO MOUSE WHOLE HIPPOCAMPUS PREPARATION

Theta (3 to 12 Hz) oscillations are the dominant network oscillations in the hippocampus, and are prominent during exploratory behaviors in rodents (Buzsáki, 2002; Buzsáki et al., 2003). Although afferent input to the hippocampus, particularly from the medial septum diagonal band of Broca, is important in generating and modulating theta activity (Stewart and Fox, 1990), the hippocampal network is capable of generating theta activity internally in the absence of external drive. This spontaneous theta activity can be recorded in the intact hippocampal isolate. A comprehensive account of this procedure was first reported by Goutagny et al. (2009), and is essential for anyone wishing to use this technique. However, a brief overview based on the authors' attempts to replicate this protocol is provided here.

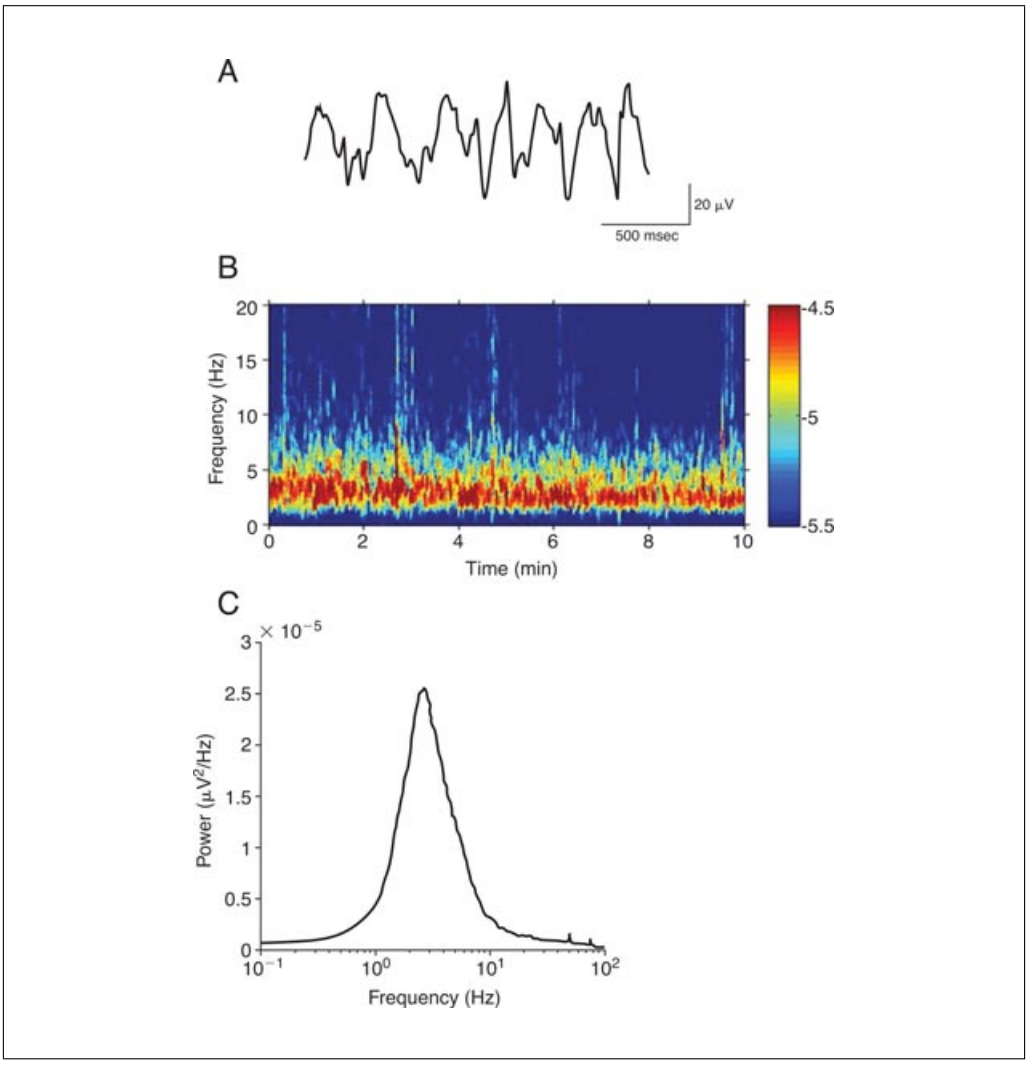

Figure 3 Spontaneous theta oscillations in the intact hippocampal isolate. (**A**) Example of spontaneous theta (3 to 12 Hz) oscillations recorded in CA1 of the intact hippocampus. The raw trace has been filtered between 1 and 20 Hz. (**B**) Spectrogram of steady-state, spontaneous theta activity in CA1 over a 10-min recording epoch. Note that in this example the peak frequency was at the lower end of the theta band as the hippocampal isolate was superfused with low K^+ (3 mM) containing aCSF. As demonstrated by Goutagny et al. (2009), the frequency of spontaneous hippocampal theta activity increases with higher K^+ concentration in the perfusate. (**C**) Fourier generated power spectrum of the recording epoch in B.

Additional Materials (also see Basic Protocol 1)

Hippocampal isolates (see Basic Protocol 1)

To record spontaneous theta activity, the intact hippocampus must be rapidly removed from the brain with minimal damage. This procedure is performed identically to hippocampal isolation for transverse slices described in Basic Protocol 1. Once isolated, the intact hippocampus should be immediately transferred to an incubation chamber filled with carbogen-bubbled aCSF and allowed to rest for ~30 min before recording. The hippocampus can be maintained relatively healthily under these conditions for several hours (3 to 4 hr).

The experimental set-up should be identical to that described in Basic Protocol 1 for submerged hippocampal slices. However, in this case, no pharmacological agent needs to be added to the perfusion solution to evoke oscillatory network activity. The hippocampal

isolate should be positioned in the recording chamber with CA1-CA3 facing vertically upwards and weights added to the extreme dorsal and ventral ends to prevent movement. The recording electrode should be inserted in CA1. Spontaneous theta activity should progressively emerge as the hippocampal tissue is incubated in the recording chamber (Fig. 3).

As with pharmacologically induced CA3 gamma oscillations, the precise amplitude and frequency of spontaneous hippocampal theta varies across the longitudinal and medial axes of CA1 (see Goutagny et al., 2009). It is therefore important to maintain a consistent electrode position across experiments, unless otherwise dictated by the experimental paradigm.

BASIC PROTOCOL 3

RECORDING OF LOCAL FIELD POTENTIALS IN MOUSE HIPPOCAMPUS IN VIVO

A protocol for chronic in vivo recording of hippocampal local field potentials (LFPs) in implanted mice is described here. It utilizes robust and economical fixed-electrode implants compatible with a range of commercial, multi-channel recording systems. This particular protocol incorporates Neuralynx (*http://www.neuralynx.com*) components, but can readily be customized to interface with alternative systems. Many more advanced electrode arrangements are available, including silicon probe-type electrodes that enable simultaneous recordings from multiple depths spanning the hippocampal axis (Buzsáki et al., 2003). Electrodes may also be attached to implanted arrays to enable post-surgical positioning and/or multiple single neuron recordings (e.g., Battaglia et al., 2009). It is also increasingly feasible to combine implanted recording electrodes with telemetry to record from un-tethered mice (e.g., Fan et al., 2011). However, the protocol described here is designed for investigators new to in vivo electrophysiology, and is particularly suitable for applications that require long-term recordings (over several months) and/or robust and small implants (e.g., pharmaco-LFP recordings). This protocol can also be combined with electromyogram (EMG) electrodes to assess mouse sleep neurophysiology.

This protocol covers construction of the recording implant, surgical technique, and the basics of LFP recording and analyses.

Materials

Cyanoacrylate glue (quick drying superglue)
Gold plating solution (e.g., non-cyanide, SIFCO Applied Surface Concepts), optional
Dental acrylic (e.g., Simplex Rapid liquid and powder, Kemdent), optional
70% ethanol
Mice
Isofluorane
Oxygen
Surgical eye lubricant (e.g., Lacri-lube, Allergan)
Lidocaine
Analgesic (e.g., buprenorphine, Buprenex)
0.9% sterile saline
Dental adhesive cement (e.g., Super-bond C&B, Sun Medical Ltd)
Silver conductive paint (e.g., Electrolube)
Gentamicin dental acrylic (e.g., DePuy International Ltd)

Delrin plastic sheet (2-mm thickness, e.g., Gilbert Curry Industrial Plastics)
Vice clamp holder (or other suitable holder for electrode array building)
Mouse stereotaxic frame

Drill press (with XYZ measuring function to ± 0.01 mm)
23-G guide cannula holders (e.g., Cooper Needle Works)
30-G stainless steel cannulae (e.g., Cooper Needle Works)
Electrode interface board (EIB; or suitable alternative)
60-μm Formvar-insulated nichrome wire (e.g., A-M Systems)
Gold pins (or other suitable method of fixing wires to selected connector chip)
Silver wire (~200-μm diameter; e.g., World Precision Instruments)
Sharp, fine scissors
Anesthesia chamber
Stereotaxic gas anesthesia mask
Homeothermic blanket and temperature probe
Fur shaver
Scalpel
Fine forceps
Surgical drill
Stainless steel skull screws (thread diameter approximately 0.75 mm; jeweller's screws may suffice)
Hypodermic needles
Sutures
Recording equipment: headstage pre-amplifier and fine wire tether cable
Computer with data acquisition software
Impedance meter (e.g., Bak Electronics IMP-2)

Construct electrode array

Figure 4 shows a schematic illustrating the main steps in construction of the array.

1. Create a Delrin platform with holes drilled at the relative distances of the stereotaxic coordinates at which the electrodes are to be implanted (diameter of the holes must accommodate the 23-G guide cannulae holders).

   Cut Delrin pieces as small as possible to minimize size and weight of the drive.

2. Insert an appropriate length of 30-G cannulae into 23-G holders. Glue into position in drilled platform holes.

   The 30-G cannulae should be cut to ~1 cm. Cut 23-G marginally longer than thickness of Delrin platform (~2 mm). Ensure 30-G is free of obstruction before gluing into place.

3. Cut out a small oblong piece of Delrin to connect the Delrin platform to the electrode interface board (EIB). Glue into position in the desired location on the Delrin platform. Glue EIB to top of the connector piece

   The Delrin connector should be as short as possible while still leaving enough room to load the wires into 30-G cannulae and connect to the EIB.

4. Cut small lengths of nichrome wire (~60-μm diameter). Insert through 30-G cannulae and make electrical connection to EIB.

   Neuralynx EIBs contain holes to facilitate the connection of wires to recording channels. The wires should be secured via the insertion of gold pins into the holes. Insertion of the pins should also strip the wire insulation, thus making the electrical connection. Alternative EIB designs may require soldering or the use of gold/silver conductive paint to make the electrical connection. Cut wire to lengths longer than needed, final trimming will be done in the last step.

5. Attach lengths of silver wire to ground and reference channels on EIB. Strip insulation before attaching and secure with gold pins.

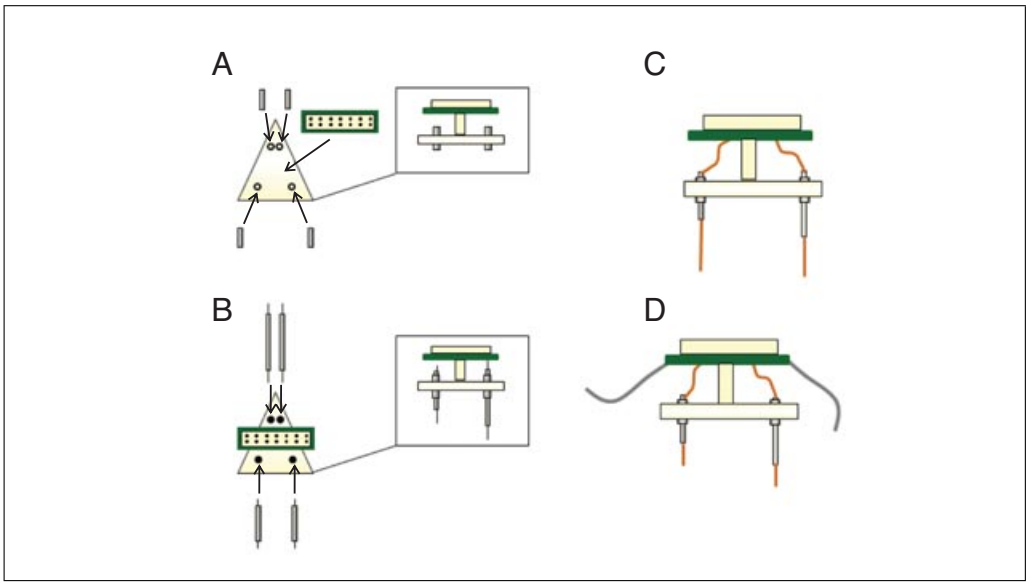

Figure 4 Schematic of array assembly. (**A**) Top-down view of holes drilled in a 2-mm thick Delrin platform, arranged according to stereotaxic coordinates; this example would target frontal cortex and hippocampus bilaterally. Lengths of 2-mm of 23-G cannulae (gray) are glued into the holes, and a connector appropriate for the headstage preamplifier is mounted in the center. (**B**) Lengths of 30-G cannulae (gray) are inserted and glued into the 23-G holders, and (**C**) lengths of nichrome wire loaded into the 30-G and connected to the electrode interface (e.g., Neuralynx EIB-18). After checking the electrical connection, the wire is glued in place at the top end of the 30-G cannulae. (**D**) Silver wire for the ground and reference connections is attached and nichrome electrode wire is then trimmed to the required lengths for implantation.

6. Check that all wires are electrically connected to the EIB. Secure wire positions by gluing around tops of 30-G cannula.

   A small amount of dental acrylic can also be applied to secure the EIB, electrode assembly, and Delrin platform. This will also facilitate handling of the array for surgery.

7. Using sharp, fine scissors, trim wires to appropriate length.

   The final wire length will depend on the depth of desired surgical implant. Deep (more ventral) electrodes should be trimmed the requisite amount longer than shallow (more dorsal) electrodes. It is generally preferable for the wire to not protrude >1.5 mm from the guide cannulae to minimize risk of damage.

8. Gold plate electrodes to an impedance of 100 to 200 KΩ at 1 KHz.

   Electrode impedance and biocompatibility are critical considerations in long-term, in vivo recordings. Nichrome wire is convenient and rigid, but bare nichrome does not produce good recordings; gold plating provides a simple and convenient means to reduce electrode impedance (which in turn improves recording quality), and gold is also relatively biologically inert. More advanced options such as poly(3,4-ethylenedioxythiophene; PEDOT) or carbon nanotubes (e.g., Ludwig et al., 2006) may be used, but are probably not necessary for basic characterization of hippocampal LFP. Platinum wires are a good alternative, though are much softer and therefore more prone to bending.

Perform surgical implant

Surgery should be carried out using sterile, aseptic, and anti-septic technique: instruments should be clean and autoclaved; contact surfaces should be washed thoroughly with 70% ethanol; a clean surgical gown or scrubs, face mask, and sterile surgical gloves should be worn; hair should be tied back and covered with a hair net. The Laboratory Animal Science Association provides useful guidelines (*http://www.lasa.co.uk/LASA_Aseptic_Surgery_2010.pdf*).

9. Weigh mouse to prepare appropriate doses of drugs and for monitoring of post-operative body weight.

10. Place mouse into anesthesia chamber. Induce anesthesia with 3% to 4% isofluorane in 100% oxygen at a delivery rate of 3 to 4 liters/min. Once mouse is deeply anesthetized, place mouse in stereotaxic frame. Use a stereotaxic gas anesthesia mask to deliver isofluorane throughout the surgery. Maintain anesthesia by inhalation of 1% to 2% isoflurane in 100% oxygen at a rate of 0.5 to 1 liter/min.

    Here, induction and maintenance of anesthesia using the inhalant anesthetic isofluorane is described. While non-inhalant anesthetics may be alternatively used (e.g., i.p. injection of a 10 mg/kg ketamine/2 mg/kg xylazine cocktail; i.p. injection of 20 ml/kg Avertin), the use of inhalant anesthetics for prolonged surgical procedures such as the one described here is strongly recommended. Protocols and standard anesthetic practice may vary by institution. Therefore, consulting the designated veterinary advisor prior to surgery is recommended.

11. Place mouse on temperature-regulated heating pad on base of stereotaxic frame for monitoring of body temperature throughout procedure and recovery. Protect eyes with Lacri-lube gel and cover. Shave head to remove hair on top of skull. Administer lidocaine to scalp. Administer analgesic. Administer 0.9% sterile saline i.p.

    Buprenex (30 μl/g body weight) injected s.c. is a good analgesic. Correct positioning of the mouse in the stereotaxic frame is crucial for successful implantation. The head should be level and securely held with limited movement in any plane. Otherwise the coordinates will be slightly off course and can result in incorrect electrode placement.

12. Using a scalpel, make incision in skin above hippocampal area. Gently dissociate tissue from skull with fine forceps and swab with sterile saline to clear skull area above hippocampus.

13. Taking care not to damage brain tissue, drill holes for support screws using a surgical drill. The holes should be no wider than the screw threads and drilled perpendicular to the skull.

    Two rostral support screws and two caudal support screws positioned over the cerebellum (caudal of Lamda) are used. Particular care should be taken when drilling the caudal screw holes due to the high concentration of blood vessels in this region. The caudal screws are also used for reference and ground connections.

14. Drill holes for electrode insertion at appropriate hippocampal stereotaxic coordinates.

    Stereotaxic coordinates should be determined using a mouse brain stereotaxic atlas.

15. Secure array in an appropriate stereotaxic holder with electrodes perpendicular to the skull. Position one hippocampal electrode directly over bregma. Use vernier scales on frame axes to adjust implant position above desired coordinates. Remove dura mater using the tip of a hooked hypodermic needle, and carefully and slowly lower electrodes to required depth using frame scale.

    Insertion of electrodes into brain should be performed gradually over several minutes to minimize tissue damage. Typical coordinates for mouse dorsal CA1 are: 2.0 mm posterior to bregma, 1.6 mm lateral to midline, and 1.3 mm ventral to brain surface (for stratum radiatum).

16. Secure array and frontal support screws to skull using dental adhesive cement. Avoid the ground and reference screws.

17. Carefully wrap array ground and reference wires around the ground and reference screws. Trim if required. Cover screws in silver conductive paint. When dry, secure these with dental adhesive cement.

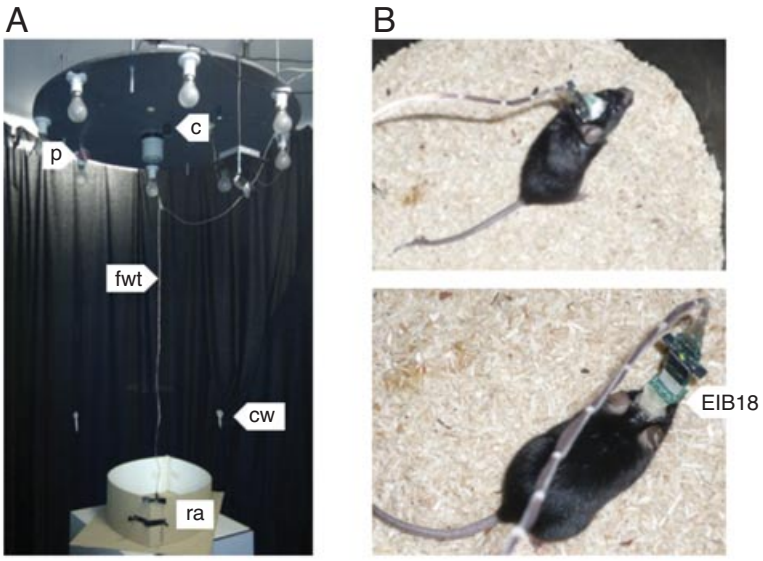

Figure 5 Overview of typical mouse LFP recording setup. (**A**) Photograph showing recording arena (ra), fine-wire tether (fwt) connected to pulleys (p) and held balanced by counterweights (cw) to allow free movement. Overhead camera (c) monitors behavior. (**B**) Implanted adult mouse connected to Neuralynx recording hardware via EIB-18 and HS18-LED.

18. Use gentamycin dental acrylic to secure the whole array assembly to the skull. Cover all exposed wires and support screws.

    Care should be taken to ensure dental acrylic is applied smoothly and evenly. Protruding pieces of dental acrylic can be smoothed off by gently rubbing with a nail file.

19. Draw skin up around dried dental acrylic. Use one suture rostral of the array and one suture caudal of the array to close the wound.

20. Remove mouse from gas anesthesia and remove from stereotaxic frame. Weigh and monitor recovery from anesthesia.

    Animal should not be deemed to have recovered from anesthesia until its self-righting reflex has returned and its body temperature has returned to normal. Implant weight combined with acrylic should be no more than 10% of animal's pre-surgery body weight. Animals should be allowed to recover for a minimum of 1 week before commencing recording.

Record LFP and analyze data

21. Connect animal to recording equipment to acquire LFP recording signal by connecting a compatible headstage pre-amplifier and associated fine wire tether cable to the array EIB. Band-pass filter the raw LFP output to remove high-frequency noise and low-frequency movement artifacts.

    Figure 5 shows an overview of a typical experimental setup. The mouse is implanted with an EIB 18 custom-made array as described in this protocol and connected to the headstage pre-amplifier. The tether must be able to move with the animal without becoming tangled to avoid noise in the recording, damage to the tether, and restriction of the animals' movements. This can be achieved by constructing a counterbalancing system composed of pulleys and weights, which allows the mouse to move freely without becoming tangled or tugging on the tether. Commutators, which connect directly to the tether, enable more free movement therefore are recommended for particularly active behavioral tasks. Commutators are available commercially with automatic or manual rotation mechanisms.

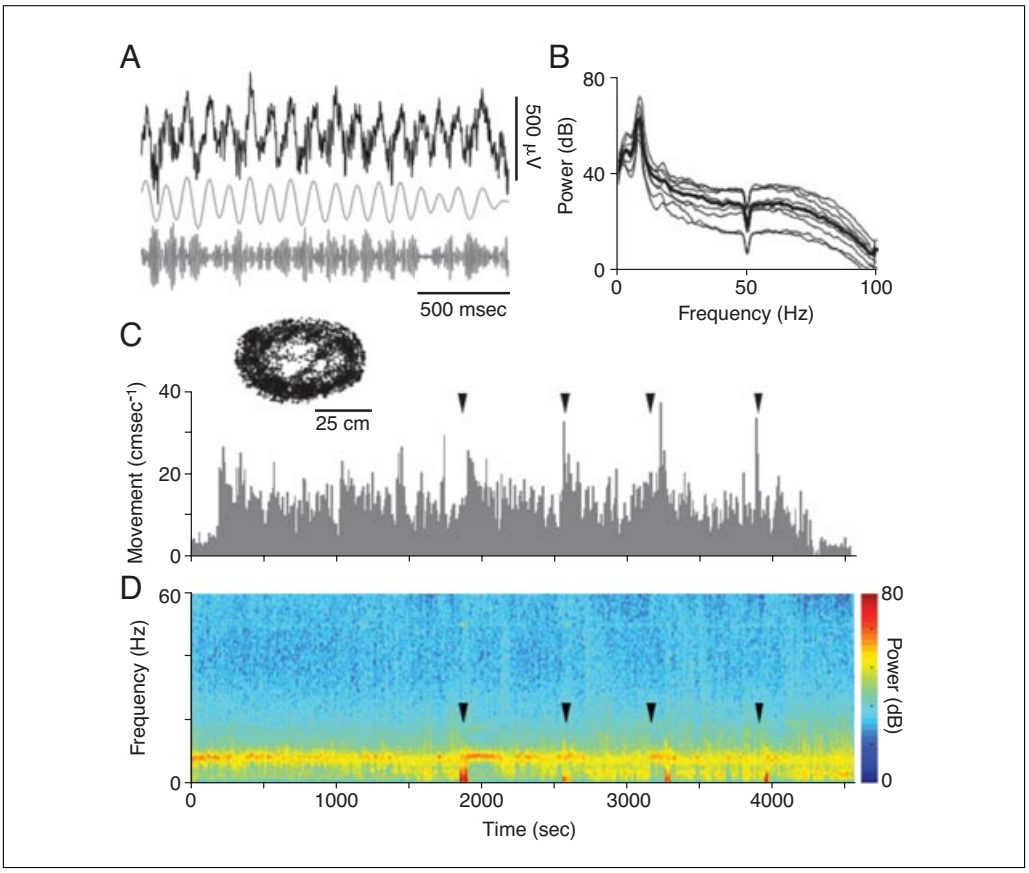

Figure 6 Examples of LFP data and spectral analysis. (**A**) 2 sec of CA1 LFP recorded during active exploration of an open field environment. Top trace shows 0.1 to 475 Hz wideband LFP, with 5 to 10 Hz (theta, middle trace) and 60 to 100 Hz (gamma, lower trace) band-pass filtered data shown below. Note characteristic correlation between gamma amplitude and theta phase. (**B**) CA1 LFP power spectra from eight adult C57BL6 mice exploring a novel environment. Thin lines show spectra for individuals, thick line shows group median. (**C**) Running speed over the course of a recording session from a single animal placed in a series of different environments at times shown by arrowheads. Speed is derived from LED-based positional tracking; inset shows raw tracking data from a single oval open field environment. (**D**) Spectrogram taken from same recording session as C, showing characteristic theta-band power at 5 to 10 Hz. Note increases in theta power coinciding with increased running speed as mouse enters different environments.

Neuralynx hardware combines with Cheetah data acquisition software, which allows the user to set the appropriate filter options, sampling frequency, and gain parameters. High-pass filter the raw LFP at 0.1 Hz and low-pass filter at 475 Hz. The sampling frequency should be set to maximize the amount of data that can be collected while maintaining a manageable file size. It is important to select a sampling frequency that will allow one to resolve all frequencies that are of interest. In general, in order to accurately reconstruct the original signal without aliasing, the sampling frequency should be set to at least double the maximum frequency of the signal that is of interest. For example, setting the sampling frequency to 1 kHz allows 500 Hz to be resolved. It is advisable to sample at the highest rate possible during recording, as the data can be downsampled offline later if necessary. The hippocampal output should contain a strong theta component, which is particularly prominent during active exploration. Figure 5 depicts a simple schematic of a typical experimental setup, and Figure 6A contains an example of raw hippocampal LFP with 4- to 10-Hz theta band indicated underneath. Compatible commutators are also available from Neuralynx.

22. Following collection of experimental LFP data, complete analysis offline.

Open source programs are available for signal processing and analysis of LFP data. These include the Chronux Toolbox (http://www.chronux.org) and EEGLab

(http://www.sccn.ucsd.edu/eeglab) software, which can be run within the MatLAB platform (MathWorks).

The types of analysis performed will ultimately depend on the experimental hypotheses and the outcomes of initial data processing. However, although this is by no means prescriptive, a typical analysis strategy would proceed through the following steps analyzing progressively higher-order features of LFP.

23. Examine raw data over long timescales to assess noise levels and remove periods with high-amplitude artifacts.
24. Examine raw data at short timescales to confirm expected characteristic features of hippocampal LFP (e.g., prominent theta power, Fig. 6B).
25. Use filtering in the time domain to select epochs or events of particular interest (e.g., periods of high amplitude theta oscillations, or detect discrete start and end times of hippocampal ripples).
26. Use Fourier analyses to quantify changes in oscillation power across frequency and time (see example spectrogram and spectra in Fig. 6).

    Multi-taper techniques offer better power estimates in non-stationary data (Bokil et al., 2007, 2010).

27. Quantify covariance of oscillations recorded at multiple sites, e.g., using Fourier coherence estimates (e.g., Jones and Wilson, 2005). Causality measures may be used to infer directed interactions (Cadotte et al., 2008; Adhikari et al., 2010).
28. Quantify cross-frequency interactions, during which the phase of one oscillation modulates the amplitude of another (Penny et al., 2008; Onslow et al., 2010).

REAGENTS AND SOLUTIONS

Use deionized, distilled water in all recipes and protocol steps.

aCSF

124 mM NaCl
3 mM KCl
24 mM $NaHCO_3$
1.25 mM NaH_2PO_4
1 mM $MgSO_4.7H_2O$
10 mM glucose
2 mM $CaCl_2$
pH 7.4 (when bubbled with 95% O_2/5% CO_2)
Osmolarity: 280 to 310 mOsm

aCSF stock can be made as a 10× working solution and diluted back to 1× in dH_2O as required. Omit $CaCl_2$ from aCSF stock and add to the working solution once it has been bubbled with carbogen (95% O_2/5% CO_2) for at least 10 min (non-carbogenated aCSF is more alkaline than pH 7.4, causing $CaCO_3$ to precipitate out of solution). The 10× aCSF stock may be stored for up to 2 weeks at 4°C.

High-sucrose cutting solution

189 mM sucrose
10 mM glucose
26 mM $NaHCO_3$
3 mM KCl
5 mM $MgSO_4.7H_2O$

continued

0.1 mM $CaCl_2$
1.25 mM NaH_2PO_4
pH 7.4 (when bubbled with 95% O_2/5% CO_2)
Osmolarity: 280 to 310 mOsm

Prepare at working concentration. Cutting solution may be prepared in bulk and stored for up to 2 weeks at 4°C. Before use, incubate in a freezer (e.g., 30 min at –20°C) to chill to ice cold.

COMMENTARY

Background Information

Hippocampal networks encompass diverse populations of neurons and interneurons, which function cooperatively to encode, store, and recall information according to current behavioral demands. Different information processing states are reflected by distinct modes of population activity, which in turn manifest as different frequencies of oscillation in hippocampal LFP (Buzsáki, 1989). For example, while a mouse actively explores a maze, 5 to 10-Hz theta rhythms generated by the synchronized activities of inhibitory and excitatory populations coordinate networks of CA3 and CA1 pyramidal neurons ('place cells') and dentate gyrus granule cells whose spike rates and times encode information about the animal's location. The theta rhythm and underlying hippocampal firing rates are coupled by characteristic temporal relationships between place cell spike-timing and the phase of the concurrent theta cycle: place cell spikes are 'phase-locked' to theta, with the spike times of a given cell consistently tending to occur around a mean preferred phase. Furthermore, the related phenomenon of phase precession means the instantaneous phase of spike-timing carries information about the animal's position in that place of the cell's firing field, and constitutes an archetypal example of temporal coding in the mammalian CNS (O'Keefe and Burgess, 2005). Given these well-characterized cellular correlates of hippocampal theta rhythms, LFP recordings demonstrating altered theta rhythmicity provide a relatively straightforward, high-throughput, and sensitive assay of neural network function.

Although it is reasonable to begin LFP analyses by focusing on oscillations at a particular frequency, neural oscillations rarely occur in splendid isolation. Again, the hippocampus has proved a powerful model system in which to study concurrent and inter-dependent oscillations: the phase of the hippocampal theta rhythm is coupled to the amplitude of local gamma-frequency oscillations (a phenomenon known as cross-frequency, or phase-amplitude coupling) in a manner that may reflect the sequential activation of hippocampal cell assemblies during mnemonic processing (Duzel et al., 2010; Onslow et al., 2010). Genetic manipulation of fast inhibitory transmission has been shown to disrupt theta-gamma coupling in CA1 (Wulff et al., 2009), hence LFP recordings and quantification of theta-gamma coupling changes can be used to infer GABA-ergic dysfunction, e.g., in mouse disease models. In this context, LFP is a particularly useful analog for comparison with clinical neurophysiology in human subjects and may uncover useful translational biomarkers of aberrant network activity.

In contrast to the theta and gamma rhythms dominant during active exploration, hippocampal LFP during quiet wakefulness and non-REM sleep is dominated by 'large irregular activity' and short ~100-msec bursts of high-frequency, 100- to 200-Hz ripple oscillations in CA3 and CA1. The cellular correlates of ripple events are well documented (Reichinnek et al., 2010), and have recently become the focus of research into circuit mechanisms of memory consolidation, which is thought to be supported by replay of sequenced activity during non-REM sleep (Sadowski et al., 2011). Again, changes in ripple properties in genetically altered mouse models exemplify the usefulness of hippocampal LFP recordings in bridging cellular and behavioral analyses (Nakashiba et al., 2009).

While the majority of hippocampal recordings target CA1, it is important to note that distinct features of the constituent hippocampal subfields are of course associated with distinct LFP signatures. These are most clearly evident in multi-site silicon probe recordings, which provide a useful guide from which to infer electrode positions in the protocol described above (see Buzsáki, 2002).

The LFP recording techniques described here are applicable to many brain regions (bearing in mind the caveats listed below), and simultaneous recordings from multiple brain

regions in behaving animals can be used to study functional interactions. Theta rhythm-mediated interactions between hippocampus and medial prefrontal cortex have been studied in this way, and provide a framework for study of network interactions during a cognition that spans humans, rats, and mice (Jones and Wilson, 2005; Siapas et al., 2005; Anderson et al., 2010; Sigurdsson et al., 2010).

Critical Parameters and Troubleshooting

The recording chamber

Two basic types of recording chambers are used for in vitro electrophysiology studies: interface and submerged. Interface chambers incubate the slice at the interface between artificial cerebrospinal fluid (aCSF), which is continuously perfused over the slice (superfused), and a highly oxygenated mist of water vapor. Under submerged conditions, the slice is bathed in a constantly perfusing stream of oxygenated aCSF.

To generate gamma oscillations in vitro, the hippocampal tissue must be provided with high levels of oxygen, as would be supplied from the blood in vivo (Hajos et al., 2009). As the interface conditions, keep the slice incubated in an oxygenated mist; the tissue is maintained sufficiently oxygenated to generate gamma activity with good signal to noise (Fisahn et al., 1998). In standard submerged recording conditions, the only source of oxygen is directly from the perfusion solution. Gamma induction under these conditions requires rapid superfusion with oxygen saturated aCSF (>5 ml/min; Mann and Paulsen, 2005; Atallah and Scanziani, 2009), although a few studies have reported induction of low-power gamma oscillations in submerged conditions with slower superfusion rates (Fisahn, 2005; Leão et al., 2009). A multiple inflow perfusion system has also been described, which further enhances bath oxygenation under submerged conditions (Hajos et al., 2009).

For basic studies, the interface approach is technically simpler and, because the required perfusion rate is slower, noise from electrode movement and perfusion currents is reduced. However, recording in interface conditions has limitations: the slice is only partially immersed in the perfusion solution, so drug compounds take longer to wash onto and off of the slice than under submerged conditions. Also, visualized patch-clamping and advanced imaging techniques can also only be performed under submerged conditions; studies that necessitate these approaches should favor a submerged recording preparation.

Basic Protocol 1: Hippocampal slice preparation and anesthesia

Although rat horizontal hippocampal slices are commonly used in studies of in vitro CA3 gamma oscillations (Buhl et al., 1998; Fisahn et al., 2004; Brown et al., 2006, 2007; Oren et al., 2006), the authors have found that horizontal slices prepared from mice to often develop spontaneous seizure-like activity following the induction of gamma oscillations (rarely have the authors found that the same is true in horizontal slices prepared from rats). Overall, the authors consider a transverse hippocampal slice preparation to most reliably generate prolonged stable gamma activity in mice. Use of this slice preparation has also been reported by multiple studies of in vitro gamma oscillations in rodents (Javedan et al., 2002; Vreugdenhil et al., 2003; Gloveli et al., 2005).

In many studies of in vitro hippocampal gamma oscillations, the animal is anesthetized with ketamine/xylazine and systemically perfused with slice cutting solution prior to brain removal and slice preparation (Lu et al.; Vreugdenhil and Toescu, 2005). In the authors' studies, it has been found that this procedure is unnecessary, slowing the speed of brain removal while affording no obvious improvement in section quality or gamma activity. However, as with the choice of recording chamber, the slice preparation will be dictated by the experimental design and experimenter's preference.

Basic Protocol 2

Bath concentrations of 50 to 500 nM kainate have been shown to reliably induce gamma oscillations in CA3 (Hajos et al., 2009), with 100 nM commonly used (Brown et al., 2006, 2007; Pietersen et al., 2009; Lu et al., 2011). The kainate concentration, perfusion rate, and type of recording chamber will influence the latency of gamma induction. Using 100 nM kainate, a perfusion rate of 2 to 3 ml/min, and interface recording conditions, typically, a gamma onset latency of 15 to 20 min is observed. Following induction, gamma power progressively increases over time until stabilizing after ~45 to 85 min (Fig. 2).

Support Protocol

The primary technical challenge for this technique lies in generating in vitro conditions capable of keeping a large volume of

tissue healthy over an extended recording period (e.g., >60 min). Interface conditions are not suitable, as only a small percentage of the tissue mass will be in contact with the perfusion solution, and as such the hippocampal isolate will rapidly die once placed into the recording chamber. Submerged recording conditions must therefore be used to ensure that the entire hippocampus is constantly bathed in oxygenated aCSF.

The induction of spontaneous theta oscillations requires extremely high oxygenation of hippocampus. To provide sufficient oxygen under submerged recording conditions, it is necessary to superfuse the tissue very rapidly with oxygen-saturated aCSF. For example, Goutagny et al. (2009) report a required superfusion rate of 26 ml/min, with theta power progressively decreasing, to a complete abolition of theta activity at 7 ml/min.

Superfusing at such a high rate generates complications for recording. Firstly, a high-speed pump is necessary to meet the demanded perfusion rate. Adaptations to the recording chamber may also be needed to minimize tissue and electrode movement from perfusion currents. A simple option is to use silicone grease to route the main flow of the perfusate around the tissue and recording electrode. The direction and strength of perfusion currents can be easily observed by adding colored dye to the perfusion solution. Standard food colorant is an inexpensive option for this purpose.

Basic Protocol 3

Hippocampal LFP signals are particularly useful given the wealth of background data linking distinct LFP features to cellular-level activity. Nevertheless, LFP must always be interpreted with care, and should always be corroborated with cellular-level (i.e., multiple single unit) recordings wherever possible, particularly when applied to less well-characterized brain regions. Key issues include the following.

Which types of neural activity contribute to LFP? LFP is dominated by slower (<300 Hz) events, namely excitatory and inhibitory post-synaptic potentials. In contrast, their rapid time course means action potentials are likely make smaller direct contributions to LFP, although of course synaptic and somatic events are typically closely linked. Given this synaptic dominance, LFP a is sometimes cited as largely reflecting input to the recording region, although local recurrent connectivity (particularly prevalent in hippocampal CA3, for example) means this may not always be the case (Pesaran, 2009).

One particularly important issue is determining the spread of LFP, hence the number of cells and synapses that contribute to a given LFP signal. Estimates of the distances of contributing neuropil from electrodes vary from tens to thousands of micrometers (Katzner et al., 2009; Kajikawa and Schroeder, 2011; Linden et al., 2011), but inevitably depend on recording region and condition, as well as the frequency and degree of synchronous activity in surrounding neural populations (Denker et al., 2011). Electrode properties (particularly size and impedance) are also an important consideration (Nelson and Pouget, 2010).

Alongside physiological contributors to LFP, passive conduction of signal by brain tissue can become a critical factor (although this may also have physiological relevance by influencing action potential timing). For example, 'hippocampal' theta can be recorded in surface EEG due to volume conduction through overlying cortex (Sirota et al., 2008). These issues come to the fore in mouse brain, where the large volume of the hippocampus and the high amplitude of its oscillations mean that avoiding hippocampus-derived LFP when recording in non-hippocampal regions may be difficult. Differential recording using a local reference electrode may help, but only if the reference signal itself is not also contaminated by passively conducted signal. In the case of hippocampal recordings, a reference electrode may be placed in white matter overlying CA1. Again, concurrent recording of multiple single unit spiking may be the only means to properly interpret LFP signals in some cases.

Since LFP and behavioral states are absolutely inter-dependent, in vivo experiments and analyses should be designed with a view to disentangling neurophysiological and behavioral effects. For example, rodent hippocampal theta power increases with the increasing running speed; fluctuations in theta power generated by changes in an animal's running movements may therefore be accounted for in the data analysis (e.g., if drug *X* increases theta power, is this due to a direct effect on hippocampal circuits, or secondary to a generalized increase in running?). This can be addressed by tracking of the animals' movements while recording; position and movement speed can then be correlated with the LFP and subsequent analyses can be performed on filtered sections of the LFP data to ensure that spectral comparisons are only made between epochs

at similar running speeds (e.g., Huxter et al., 2007).

The two main sources of non-neurophysiological noise during in vivo LFP recordings are animal/tether movement and 50 Hz or 60 Hz contamination produced by mains electricity. Streamlining array design and using a counterbalanced pulley system to regulate the length and tension of the recording tether are useful in minimizing noise generated by cable movement. Designing recording environments to minimize collisions between array/tether and objects can also help. Chewing and grooming can produce artifacts, although differential recording with a local reference should minimize these; using liquid rewards in behavioral tasks can also help. Mains noise can be minimized by turning off unessential electrical equipment in the vicinity of the recording hardware, shielding the testing area with a Faraday cage, and grounding all electrical equipment to a common ground.

On-line filtering could be used to reject noise and can be used for visualization purposes, but it is advisable not to filter saved data (which risks discarding useful signal), but to use subsequent software filters if necessary. It is essential that LFP sampling frequency and any on-line filter settings accommodate all frequencies of potential interest. In a hippocampal context, the highest frequency LFP features documented to date (ripples) typically do not exceed 300 Hz, so sampling frequencies of ∼1 KHz should be sufficient.

Anticipated Results

Typical hippocampal LFP traces and examples of common data analyses are shown in Figure 6. Analyses of this type are ideal for a first look at the data. The results obtained will influence further signal processing that may be performed but is beyond the scope of this protocol.

Time Considerations

The in vitro slice and whole hippocampal preparations are acute and rapid. For the in vivo experiments, array construction, surgical implantation, and recovery will delay the collection of experimental data, but this protocol is designed for long-term studies and large volumes of data can be collected from individual mice. Preparation and implantation of a cohort of six mice should take ∼1 week. At least 7 days should be allowed for full post-surgical recovery prior to starting recording. Analysis of large volumes of LFP data can also be time consuming, though existing software do speed up the process considerably.

Literature Cited

Adhikari, A., Sigurdsson, T., Topiwala, M.A., and Gordon, J.A. 2010. Cross-correlation of instantaneous amplitudes of field potential oscillations: A straightforward method to estimate the directionality and lag between brain areas. *J. Neurosci. Methods* 191:191-200.

Anderson, K.L., Rajagovindan, R., Ghacibeh, G.A., Meador, K.J., and Ding, M. 2010. Theta oscillations mediate interaction between prefrontal cortex and medial temporal lobe in human memory. *Cereb. Cortex* 20:1604-1612.

Arguello, P.A. and Gogos, J.A. 2006. Modeling madness in mice: One piece at a time. *Neuron* 52:179-196.

Atallah, B.V. and Scanziani, M. 2009. Instantaneous modulation of gamma oscillation frequency by balancing excitation with inhibition. *Neuron* 62:566-577.

Battaglia, F.P., Kalenscher, T., Cabral, H., Winkel, J., Bos, J., Manuputy, R., van Lieshout, T., Pinkse, F., Beukers, H., and Pennartz, C. 2009. The Lantern: An ultra-light micro-drive for multi-tetrode recordings in mice and other small animals. *J. Neurosci. Methods* 178:291-300.

Bokil, H., Purpura, K., Schoffelen, J.M., Thomson, D., and Mitra, P. 2007. Comparing spectra and coherences for groups of unequal size. *J. Neurosci. Methods* 159:337-345.

Bokil, H., Andrews, P., Kulkarni, J.E., Mehta, S., and Mitra, P.P. 2010. Chronux: A platform for analyzing neural signals. *J. Neurosci. Methods* 192:146-151.

Brown, J.T., Teriakidis, A., and Randall, A.D. 2006. A pharmacological investigation of the role of GLUK5-containing receptors in kainate-driven hippocampal gamma band oscillations. *Neuropharmacology* 50:47-56.

Brown, J.T., Davies, C.H., and Randall, A.D. 2007. Synaptic activation of GABAB receptors regulates neuronal network activity and entrainment. *Eur. J. Neurosci.* 25:2982-2990.

Buhl, E.H., Tamás, G., and Fisahn, A. 1998. Cholinergic activation and tonic excitation induce persistent gamma oscillations in mouse somatosensory cortex in vitro. *J. Physiol.* 513:117-126.

Buzsáki, G. 1989. Two-stage model of memory trace formation: A role for "noisy" brain states. *Neuroscience* 31:551-570.

Buzsáki, G. 2002. Theta oscillations in the hippocampus. *Neuron* 33:325-340.

Buzsáki, G., Buhl, D.L., Harris, K.D., Csicsvari, J., Czeh, B., and Morozov, A. 2003. Hippocampal network patterns of activity in the mouse. *Neuroscience* 116:201-211.

Cadotte, A.J., DeMarse, T.B., He, P., and Ding, M. 2008. Causal measures of structure and plasticity in simulated and living neural networks. *PloS One* 3:e3355.

Denker, M., Roux, S., Linden, H., Diesmann, M., Riehle, A., and Grun, S. 2011. The local field potential reflects surplus spike synchrony. *Cereb. Cortex* 21:2681-2695.

Duzel, E., Penny, W.D., and Burgess, N. 2010. Brain oscillations and memory. *Curr. Opin. Neurobiol.* 20:143-149.

Fan, D., Rich, D., Holtzman, T., Ruther, P., Dalley, J.W., Lopez, A., Rossi, M.A., Barter, J.W., Salas-Meza, D., Herwik, S., Holzhammer, T., Morizio, J., and Yin, H.H. 2011. A wireless multi-channel recording system for freely behaving mice and rats. *PloS One* 6:e22033.

Fisahn, A. 2005. Kainate receptors and rhythmic activity in neuronal networks: Hippocampal gamma oscillations as a tool. *J. Physiol.* 562:65-72.

Fisahn, A., Pike, F.G., Buhl, E.H., and Paulsen, O. 1998. Cholinergic induction of network oscillations at 40[thinsp]Hz in the hippocampus in vitro. *Nature* 394:186-189.

Fisahn, A., Contractor, A., Traub, R.D., Buhl, E.H., Heinemann, S.F., and McBain, C.J. 2004. Distinct roles for the kainate receptor subunits GluR5 and GluR6 in kainate-induced hippocampal gamma oscillations. *J. Neurosci.* 24:9658-9668.

Gloveli, T., Dugladze, T., Rotstein, H.G., Traub, R.D., Monyer, H., Heinemann, U., Whittington, M.A., and Kopell, N.J. 2005. Orthogonal arrangement of rhythm-generating microcircuits in the hippocampus. *Proc. Natl. Acad. Sci. U.S.A.* 102:13295-13300.

Goutagny, R., Jackson, J., and Williams, S. 2009. Self-generated theta oscillations in the hippocampus. *Nat. Neurosci.* 12:1491-1493.

Hajos, N., Ellender, T.J., Zemankovics, R., Mann, E.O., Exley, R., Cragg, S.J., Freund, T.F., and Paulsen, O. 2009. Maintaining network activity in submerged hippocampal slices: Importance of oxygen supply. *Eur. J. Neurosci.* 29:319-327.

Huxter, J.R., Zinyuk, L.E., Roloff, E.L., Clarke, V.R., Dolman, N.P., More, J.C., Jane, D.E., Collingridge, G.L., and Muller, R.U. 2007. Inhibition of kainate receptors reduces the frequency of hippocampal theta oscillations. *J. Neurosci.* 27:2212-2223.

Javedan, S.P., Fisher, R.S., Eder, H.G., Smith, K., and Wu, J. 2002. Cooling abolishes neuronal network synchronization in rat hippocampal slices. *Epilepsia* 43:574-580.

Jones, M.W. and Wilson, M.A. 2005. Theta rhythms coordinate hippocampal-prefrontal interactions in a spatial memory task. *PLoS Biol.* 3:e402.

Kajikawa, Y. and Schroeder, C.E. 2011. How local is the local field potential. *Neuron* 72:847-858.

Katzner, S., Nauhaus, I., Benucci, A., Bonin, V., Ringach, D.L., and Carandini, M. 2009. Local origin of field potentials in visual cortex. *Neuron* 61:35-41.

Klausberger, T. and Somogyi, P. 2008. Neuronal diversity and temporal dynamics: The unity of hippocampal circuit operations. *Science* 321:53-57.

Korotkova, T., Fuchs, E.C., Ponomarenko, A., von Engelhardt, J., and Monyer, H. 2010. NMDA receptor ablation on parvalbumin-positive interneurons impairs hippocampal synchrony, spatial representations, and working memory. *Neuron* 68:557-569.

Leão, R.N., Tan, H.M., and Fisahn, A. 2009. Kv7/KCNQ channels control action potential phasing of pyramidal neurons during hippocampal gamma oscillations in vitro. *J. Neurosci.* 29:13353-13364.

Linden, H., Tetzlaff, T., Potjans, T.C., Pettersen, K.H., Grun, S., Diesmann, M., and Einevoll, G.T. 2011. Modeling the spatial reach of the LFP. *Neuron* 72:859-872.

Lu, C.B., Jefferys, J.G.R., Toescu, E.C., and Vreugdenhil, M. 2011. In vitro hippocampal gamma oscillation power as an index of in vivo CA3 gamma oscillation strength and spatial reference memory. *Neurobiol. Learn. Mem.* 95:221-230.

Ludwig, K.A., Uram, J.D., Yang, J., Martin, D.C., and Kipke, D.R. 2006. Chronic neural recordings using silicon microelectrode arrays electrochemically deposited with a poly(3,4-ethylenedioxythiophene) (PEDOT) film. *J. Neur. Eng.* 3:59-70.

Mann, E.O. and Paulsen, O. 2005. Mechanisms underlying gamma ([γ]40 Hz') network oscillations in the hippocampus—A mini-review. *Prog. Biophys. Mol. Biol.* 87:67-76.

Mann, E.O. and Mody, I. 2010. Control of hippocampal gamma oscillation frequency by tonic inhibition and excitation of interneurons. *Nat. Neurosci.* 13:205-212.

Nakashiba, T., Buhl, D.L., McHugh, T.J., and Tonegawa, S. 2009. Hippocampal CA3 output is crucial for ripple-associated reactivation and consolidation of memory. *Neuron* 62:781-787.

Nelson, M.J. and Pouget, P. 2010. Do electrode properties create a problem in interpreting local field potential recordings? *J. Neurophysiol.* 103:2315-2317.

O'Keefe, J. and Burgess, N. 2005. Dual phase and rate coding in hippocampal place cells: Theoretical significance and relationship to entorhinal grid cells. *Hippocampus* 15:853-866.

Onslow, A.C., Bogacz, R., and Jones, M.W. 2010. Quantifying phase-amplitude coupling in neuronal network oscillations. *Prog. Biophys. Mol. Biol.* 105:49-57.

Oren, I., Mann, E.O., Paulsen, O., and Hájos, N. 2006. Synaptic currents in anatomically identified CA3 neurons during hippocampal gamma oscillations in vitro. *J. Neurosci.* 26:9923-9934.

Penny, W.D., Duzel, E., Miller, K.J., and Ojemann, J.G. 2008. Testing for nested oscillation. *J. Neurosci. Methods* 174:50-61.

Pesaran, B. 2009. Uncovering the mysterious origins of local field potentials. *Neuron* 61:1-2.

Pietersen, A.N., Patel, N., Jefferys, J.G., and Vreugdenhil, M. 2009. Comparison between spontaneous and kainate-induced gamma

oscillations in the mouse hippocampus in vitro. *Eur. J. Neurosci.* 29:2145-2156.

Reichinnek, S., Kunsting, T., Draguhn, A., and Both, M. 2010. Field potential signature of distinct multicellular activity patterns in the mouse hippocampus. *J. Neurosci.* 30:15441-15449.

Sadowski, J.H., Jones, M.W., and Mellor, J.R. 2011. Ripples make waves: Binding structured activity and plasticity in hippocampal networks. *Neur. Plast.* 2011:960389.

Siapas, A.G., Lubenov, E.V., and Wilson, M.A. 2005. Prefrontal phase locking to hippocampal theta oscillations. *Neuron* 46:141-151.

Sigurdsson, T., Stark, K.L., Karayiorgou, M., Gogos, J.A., and Gordon, J.A. 2010. Impaired hippocampal-prefrontal synchrony in a genetic mouse model of schizophrenia. *Nature* 464:763-767.

Sirota, A., Montgomery, S., Fujisawa, S., Isomura, Y., Zugaro, M., and Buzsaki, G. 2008. Entrainment of neocortical neurons and gamma oscillations by the hippocampal theta rhythm. *Neuron* 60:683-697.

Stewart, M. and Fox, S.E. 1990. Do septal neurons pace the hippocampal theta rhythm. *Trends Neurosci.* 13:163-169.

Vreugdenhil, M., Jefferys, J.G.R., Celio, M.R., and Schwaller, B. 2003. Parvalbumin-deficiency facilitates repetitive IPSCs and gamma oscillations in the hippocampus. *J. Neurophysiol.* 89:1414-1422.

Vreugdenhil, M. and Toescu, E.C. 2005. Age-dependent reduction of gamma oscillations in the mouse hippocampus in vitro. *Neuroscience* 132:1151-1157.

Wulff, P., Ponomarenko, A.A., Bartos, M., Korotkova, T.M., Fuchs, E.C., Bahner, F., Both, M., Tort, A.B., Kopell, N.J., Wisden, W., and Monyer, H. 2009. Hippocampal theta rhythm and its coupling with gamma oscillations require fast inhibition onto parvalbumin-positive interneurons. *Proc. Natl. Acad. Sci. U.S.A.* 106:3561-3566.